

## Self-Assembly and Self-Metallization of Porphyrin Nanosheets

Zhongchun Wang,<sup>†</sup> Zhiyong Li,<sup>‡</sup> Craig J. Medforth,<sup>†</sup> and John A. Shelnutt<sup>\*,†,§</sup>

*Nanostructure and Semiconductor Physics Department, Sandia National Laboratories, Albuquerque, New Mexico 87185, Quantum Science Research, Hewlett-Packard Laboratories, 1501 Page Mill Road, Palo Alto, California 94304, and Department of Chemistry, University of Georgia, Athens, Georgia 30602*

Received November 17, 2006; E-mail: jasheln@unm.edu

The self-assembly approach has been widely adopted in the effort to design and prepare functional materials.<sup>1</sup> Porphyrins are particularly attractive building blocks for self-assembly because the intimate packing of these aromatic macrocycles can result in rich photophysical and photochemical properties that are important in many technological applications. Covalent or noncovalent porphyrinic assemblies have been used to model the solar energy capture and transfer processes seen in naturally occurring photosystems, as well as to create artificial photoactive molecular devices.<sup>2</sup> Recently, we have exploited the ionic self-assembly of oppositely charged porphyrin tectons to synthesize porphyrin nanotubes<sup>3a,b</sup> in aqueous solution and porphyrin nanofiber bundles<sup>3c</sup> in an aqueous–organic two-phase system, with the ultimate goal of making novel photoactive nanodevices.

Herein, we describe the synthesis of discrete free-standing porphyrin nanosheets using a reprecipitation method. This method has been widely adopted in the synthesis of organic nanoparticles<sup>4a,b</sup> and recently by Hu et al.<sup>4c</sup> in the surfactant-assisted synthesis of hollow hexagonal nanoprisms from Zn 5,10,15,20-tetra(4-pyridyl)-porphyrin. While many two-dimensional (2-D) inorganic nanostructures (e.g., titania nanosheets exfoliated from bulk materials<sup>5</sup>) have been synthesized and studied, there have been only a few attempts to make well-defined 2-D organic nanostructures. One example is the square platelets<sup>6</sup> formed by controlled crystallization of polystyrene–poly(ethylene oxide) (PS–PEO) diblock copolymers in methylcyclohexane. Others include polymer nanosheets or nanofilms with a 2-D hydrogen-bonding network prepared on planar substrates using the Langmuir–Blodgett technique.<sup>7</sup> However, these organic structures<sup>6,7</sup> do not possess the diverse photophysical and photochemical properties possible with porphyrin-based systems.

In a typical synthesis of the porphyrin nanosheets, 200  $\mu\text{L}$  of a 1.0 mM solution of Sn(IV) 5-(4-pyridyl)-10,15,20-triphenyl-porphyrin dichloride (SnPyTriPP; Figure 1e, inset) in ethanol was injected into 10 mL of deionized water at room temperature under vigorous stirring. A translucent greenish-pink colloid was obtained after stirring for approximately 10 min. Using atomic force microscopy (AFM), transmission electron microscopy (TEM), and scanning electron microscopy (SEM), the colloidal porphyrin particles prepared were revealed to be a collection of nanosheets (Figure 1). The square nanosheets occur with a range of edge lengths (0.3–1  $\mu\text{m}$ ), as can be best seen in Figure 1c and in the Supporting Information Figure S1. However, they possess a fairly uniform thickness of 7–12 nm (see Figure 1d) giving aspect ratios up to 100. Interestingly, a triangular sheet lies along the diagonal of the square on ca. 30% of the nanosheets (Figure 1a,c and Figure S1).

The self-assembly of SnPyTriPP was also investigated using other conditions and found to produce different nanostructures.

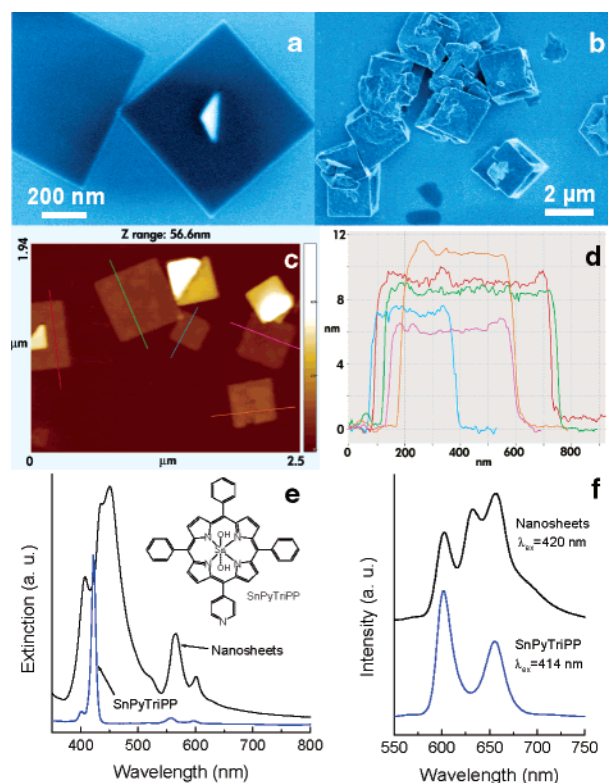


**Figure 1.** (a) SEM image of SnPyTriPP nanosheets on Si(100) substrate; (b) SEM image of porphyrin “cubes” on Si(100); (c) AFM image of porphyrin nanosheets adsorbed on Si(100); (d) height profiles of the lines in panel c, showing that the nanosheets have thicknesses of 7–12 nm, independent of their side lengths; (e) UV–visible extinction and (f) emission spectra of aqueous suspensions of the nanosheets. The absorption (e) and emission (f) spectra of monomeric SnPyTriPP in ethanol are also shown for comparison. Inset in panel e shows the molecular structure of SnPyTriPP (OH axial ligands are shown as these are expected to be present in neutral aqueous solution).

Cubic microstructures with hollow faces (Figures 1b, S2) were obtained by injecting the precursor ethanol solution into hot water ( $\sim 90$  °C) and letting the mixture cool. Nanosheets like those in Figure 1a,c but with slightly shorter average edge lengths were obtained using chilled water ( $\sim 4$  °C) (data not shown). Methanol could also be used as the porphyrin solvent in the self-assembly process, with little change in the product size distribution at room temperature.

The shape and sharp edges of the porphyrin nanosheets suggest that they might be single crystals. A crystalline structure is also suggested by powder X-ray diffraction (XRD) measurements of the nanosheets cast onto a Si(100) substrate (Figure S3). Although the nanosheets show far fewer peaks than the powder of the SnPyTriPP(Cl)<sub>2</sub> precursor, all the peaks in the XRD pattern of the nanosheets are observed for the porphyrin precursor powder. The

<sup>†</sup> Sandia National Laboratories.

<sup>‡</sup> Hewlett-Packard Laboratories.

<sup>§</sup> University of Georgia.

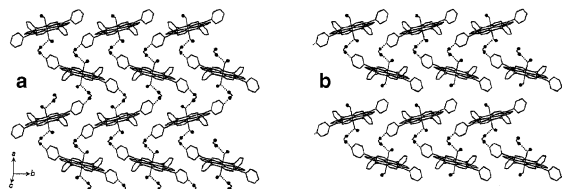


**Figure 2.** (a) Crystal structure of  $\text{Sn}(\text{OH})_2\text{TPyP}$  showing the hydrogen-bonding network ( $\text{Sn}-\text{O}\cdots\text{H}-\text{O}-\text{H}\cdots\text{N}$ ) between molecules<sup>9</sup> and (b) a related hydrogen-bonding network for the  $\text{Sn}(\text{OH})_2\text{PyTriPP}$  nanosheets.

markedly different XRD patterns may be related to the nanoscale thickness of the sheets and their orientation on the substrate. No long-range periodicity was observed in either the precursor powder or the nanosheets as indicated by the absence of significant diffraction peaks in the low-angle region (inset of Figure S3).

As expected for a multi-porphyrin system, the porphyrin nanosheets exhibit absorption and emission spectra that are more complicated than those of the monomers.<sup>4b,8</sup> Compared to monomeric  $\text{SnPyTriPP}$  in ethanol, which shows a Soret band at 422 nm and Q-bands at 558 and 598 nm, the extinction spectrum of the nanosheets is more complex (Figure 1e). The Soret band is split into a blue-shifted band at 408 nm and two red-shifted bands at 436 and 450 nm, while the Q-bands red shift slightly to 566 and 602 nm. The emission spectrum of the nanosheets (Figure 1f) shows four bands at 602, 632, 656, and 693 nm, while only two bands at 602 and 656 nm are seen for monomeric  $\text{SnPyTriPP}$ .

With regards to the mechanism of formation of the nanosheets, it is possible that hydrogen bonding between the axial hydroxyl ligand of a  $\text{Sn}(\text{OH})_2\text{PyTriPP}$  molecule and the pyridyl group of an adjacent molecule (perhaps via a bridging water molecule) might be involved in the self-assembly of the nanosheets (Figure 2). Such a network of  $\text{Sn}-\text{O}\cdots\text{H}-\text{O}-\text{H}\cdots\text{N}$  hydrogen bonds is known to occur in tin tetra(pyridyl)porphyrin crystal structures (Figure 2a).<sup>9</sup> Together with hydrophobic forces and  $\pi-\pi$  interactions, such a network might lead to formation of the nanosheets. Direct coordination between  $\text{Sn}(\text{IV})$  and the pyridyl groups is not expected since  $\text{Sn}(\text{IV})$  has a weak affinity for pyridyl groups.<sup>10</sup> Injecting the  $\text{SnPyTriPP}$  ethanol solution into water at pH 2, where the pyridyl groups will become fully protonated, yields no well-defined aggregates, supporting the idea that pyridine acts as a hydrogen-bond acceptor in such a network.

Similar to the  $\text{Sn}$ -porphyrin containing nanotubes,<sup>3b</sup> the nanosheets formed from  $\text{SnPyTriPP}$  retain the solution photocatalytic properties of  $\text{Sn}$  porphyrins, as shown by their self-metallization reactions. A colloidal suspension containing the nanosheets, ascorbic acid (10 mM) and  $\text{K}_2\text{PtCl}_4$  (0.1 mM) was exposed to incandescent light from a projector lamp ( $800 \text{ nmol cm}^{-2} \text{ s}^{-1}$ ) for 6.5 min and then kept in the dark overnight ( $\sim 14 \text{ h}$ ). Immediately after the light exposure, the suspension was still a colloid, but after overnight storage the nanosheets had turned black and settled out. Figure 3a shows a porphyrin nanosheet decorated with 2–6 nm Pt nanoparticles and dendrites grown photocatalytically<sup>11</sup> on its surface during the 6.5 min of light exposure. Figures 3b and S4 show the effects of letting the Pt seeds grow further autocatalytically<sup>11</sup> in the dark until all of the Pt salt in the reaction mixture is consumed. This results in heavily metallized “pizza-box” porphyrin–Pt composite nanostructures that might be promising for electrocatalytic applications. In a similar way, the porphyrin nanosheets can be self-metallized with other metals such as Pd and Au (data not shown).

The unmetallized nanosheets can be selectively deposited onto the cathode during electrophoresis, indicating that they may have a positively charged surface. They also readily adsorb onto various substrates such as Si, Au, glassy carbon, and highly ordered

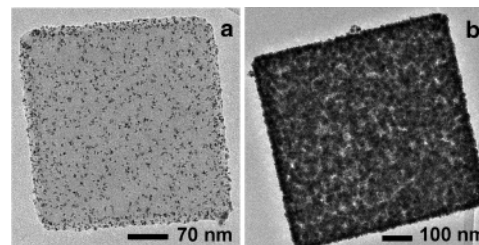


**Figure 3.** TEM images of (a) a  $\text{SnPyTriPP}$  nanosheet decorated with photodeposited Pt nanoparticles and (b) a nanosheet encased within a thin porous Pt mat of autocatalytically grown Pt dendrites. Note in Supporting Information Figures S4 and S5 that all the triangular sheets were platinized along with the squares.

pyrolytic graphite. Photometallization of nanosheets previously adsorbed on the substrate (see Figures S5 and S6) suggests that the fabrication of nanoelectrodes with ohmic contacts between the metal and the nanosheets may be possible. This might facilitate the integration of the porphyrin nanosheets into optoelectronic nanodevices.

In summary, square porphyrin nanosheets with high aspect ratios have been synthesized for the first time. Their unique morphology, photocatalytic properties, and large surface areas suggest that they may find a wide range of applications in electronics, photonics, and catalytic systems. We are currently investigating the electrical properties of the nanosheets using AFM on conducting substrates and evaluating their potential applications in electronic and optoelectronic nanodevices.

**Acknowledgment.** This work was partially supported by U.S. DOE Grant DE-FG02-02ER15369 (J.A.S.) and DARPA (Z.L.). Sandia is a multiprogram laboratory operated by Sandia Corporation, a Lockheed-Martin company, for the U.S. Department of Energy’s National Nuclear Security Administration under Contract DE-ACO4-94AL85000. We thank Dr. K. J. Ho at UNM for the fluorescence measurements.

**Supporting Information Available:** Experimental details, XRD data, and additional AFM, SEM, and TEM images of the nanosheets. This material is available free of charge via the Internet at <http://pubs.acs.org>.

## References

- Lehn, J.-M. *Angew. Chem., Int. Ed.* **1990**, *29*, 1304.
- (a) Crossley, M. J.; Burn, P. L. *Chem. Commun.* **1991**, 1569. (b) Tsuda, A.; Osuka, A. *Science* **2001**, *293*, 79. (c) Drain, C. M.; Goldberg, I.; Sylvain, I.; Falber, A. *Top. Curr. Chem.* **2005**, *245*, 55. (d) Elemans, J. A. A. W.; van Hameren, R.; Nolte, R. J. M.; Rowan, A. E. *Adv. Mater.* **2006**, *18*, 1.
- (a) Wang, Z.; Medforth, C. J.; Shelnett, J. A. *J. Am. Chem. Soc.* **2004**, *126*, 15955. (b) Wang, Z.; Medforth, C. J.; Shelnett, J. A. *J. Am. Chem. Soc.* **2004**, *126*, 16720. (c) Wang, Z.; Ho, K. J.; Medforth, C. J.; Shelnett, J. A. *Adv. Mater.* **2006**, *18*, 2557.
- (a) Xiao, D.; Xi, L.; Yang, W.; Fu, H.; Shuai, Z.; Fang, Y.; Yao, J. *J. Am. Chem. Soc.* **2003**, *125*, 6740. (b) Gong, X.; Milic, T.; Xu, C.; Bateas, J. D.; Drain, C. M. *J. Am. Chem. Soc.* **2002**, *124*, 14290. (c) Hu, J.-S.; Guo, Y.-G.; Liang, H.-P.; Wan, L.-J.; Jiang, L. *J. Am. Chem. Soc.* **2005**, *127*, 17090.
- Sasaki, T.; Watanabe, M.; Hashizume, H.; Yamada, H.; Nakazawa, H. *J. Am. Chem. Soc.* **1996**, *118*, 8329.
- (a) Gast, A. P.; Vinson, P. K.; Cogan-Farinast, K. A. *Macromolecules* **1993**, *26*, 1774. (b) Riess, G. *Prog. Polym. Sci.* **2003**, *28*, 1107.
- (a) Taniguchi, T.; Yokoyama, Y.; Miyashita, T. *Macromolecules* **1997**, *30*, 3646. (b) Matsui, J.; Mitsuishi, M.; Aoki, A.; Miyashita, T. *J. Am. Chem. Soc.* **2004**, *126*, 3708.
- (a) Hunter, C. A.; Sanders, J. K. M.; Stone, A. J. *Chem. Phys.* **1989**, *133*, 395. (b) Sendt, K.; Johnston, L. A.; Hough, W. A.; Crossley, M. J.; Hush, N. S.; Reimers, J. R. *J. Am. Chem. Soc.* **2002**, *124*, 9299.
- Jo, H. J.; Jung, S. H.; Kim, H.-J. *Bull. Korean Chem. Soc.* **2004**, *25*, 18693.
- Kim, H.-J.; Jo, H. J.; Kim, J.; Kim, S.-Y.; Kim, D.; Kim, K. *CrystEngComm* **2005**, *7*, 417.
- Song, Y.; Yang, Y.; Medforth, C. J.; Pereira, E.; Singh, A. K.; Xu, H.; Jiang, Y.; Brinker, C. J.; van Swol, F.; Shelnett, J. A. *J. Am. Chem. Soc.* **2004**, *126*, 635.

JA0682500